In vitro exosomal transfer of Nrf2 led to the oxaliplatin resistance in human colorectal cancer LS174T cells

Peer-reviewed author version

Mostafazadeh, Mostafa; KAHROBA, Houman; Haiaty, Sanya; TazeKand, Abbas P.; Samadi, Nasser; Rahbarghazi, Reza & Nouri, Mohammad (2022) In vitro exosomal transfer of Nrf2 led to the oxaliplatin resistance in human colorectal cancer LS174T cells. In: CELL BIOCHEMISTRY AND FUNCTION,.

DOI: 10.1002/cbf.3703
Handle: http://hdl.handle.net/1942/37398

In vitro exosomal transfer of Nrf2 led to the oxaliplatin resistance in human colorectal cancer LS174T cells

Abstract

Chemotherapy resistance is a serious pitfall in the treatment of colon cancers. Previous studies have found that exosomes (Exo) display a pivotal role in tumor drug resistance via engaging active proteins and genetic materials in the acceptor cells. To date, mechanisms orchestrating Exo-derived resistance in cancer cells are the center of attention. Herein, we aimed to evaluate the role of exosomal Nrf2 on oxaliplatin resistance in human colorectal cancer LS174T cells *in vitro*. To this end, exosomal-Nrf2-mediated oxaliplatin resistance was examined using different assays. Exo were isolated from resistant LS174T cells (LS174T/R) and co-cultured on sensitive LS174T cells (LS174T/S).

According to our data, LS174T/S cells successfully adsorbed PKH26-Exo driven from LS174T/R cells. Western blotting showed an increased Nrf2 level in Exo isolated from LS174T/R cells compared to LS174T/S cell-derived Exo ($p<0.05$). The incubation of LS174T/S cells with LS174T/R-derived Exo increased IC50 values in the presence of oxaliplatin ($p<0.05$). Besides, the apoptotic changes were diminished in LS174T/S cells after incubation with LS174T/R-derived Exo. Of note, the exposure of LS174T/S cells to LS174T/S cell-derived Exo indicated the expression of Nrf2 and P-gp compared to the control group ($p<0.05$). In line with these changes, lower intracellular Rhodamin123 content was detected in Exo-treated cells compared to the control group. Exo increased migration and clonogenic capacity of LS174T/S cells after incubation with Exo-derived from resistant cells. Of note, inhibition of Nrf2 with a specific blocker, brusatol, blunted these effects.

Taken together, Exo-mediated transfer of Nrf2 is involved in the development of oxaliplatin resistance in colon cancer cells by up-regulating P-gp.

Keywords: Human Colorectal Cancer LS174T Cells; Chemoresistance; Exosomes; Nrf2; Oxaliplatin

1. Introduction

Colon cancer (CC) is the third most frequently diagnosed malignancy in both sexes worldwide and the second leading cause of cancer-related deaths [1]. Oxaliplatin (1-OHP), a third-generation platinum analog that interferes with DNA synthesis and RNA transcription through inter-and intra-strand platinum-DNA adducts, is widely used as the first-line treatment for advanced CC. The combination of oxaliplatin with l-leucovorin and 5-fluorouracil (FOLFOX) is applied to enhance the chemotherapy success rate to more than 50%. This combination therapy increases the overall survival time of CC patients by about 2 years for metastatic CC [2]. Unfortunately, more than 50% of stage II and III CC patients show resistance to oxaliplatin-based chemotherapy, which limits therapeutic efficacy [3]. Hence, it's imperative to study the molecular mechanisms of oxaliplatin resistance to develop novel therapeutic strategies to benefit CC patients.

The interplay between tumor cells within the tumor microenvironment (TME) is one of the potential mechanisms for spreading the chemoresistance factors that have recently received abundant attention. [4]. Exosomes (Exo) are a subset of extracellular vesicles with sizes ranging from 40 to 150 nm. Exo possess a double-layered lipid membrane and harbor multi-signal (RNAs, DNA, lipids, and functional proteins). It is thought that Exo have a critical role in paracrine interaction between the cells from similar or different lineages [5, 6]. Following the onset of CC, the release of Exo from tumor cells partakes in tumor initiation, progression. Meanwhile, the presence of Exo in the tumor niche and the active interplay between cells contribute to chemotherapy resistance mediated by sharing bioactive molecules to recipient cells [7]. Although the role of the genetic factors has been well-documented in the chemotherapeutic resistance of CC cells, however, the potential role of exosomal proteins in chemoresistance is less lacking [8].

Nuclear factor erythroid 2-related factor 2 (Nrf2), which belongs to the Cap-n-Collar family of basic leucine zipper proteins, is a key transcriptional factor that acts as a master regulator of cellular redox homeostasis [9]. In response to endogenous and exogenous stresses, Nrf2 detaches from Kelch-like ECH-associated protein 1 (Keap1) and translocates to the nucleus to bind to the antioxidant response elements (ARE) in

the regulatory region of the genes to increase their expression levels. ARE positive genes include phase II detoxifying enzymes and ATP-dependent drug efflux pumps [10]. Previously, it has been reported that Nrf2 is abnormally overexpressed in CC and its up-regulation is associated with chemotherapy resistance [11-13]. However, the role of exosomal Nrf2 in oxaliplatin resistance in CC remains unknown. Therefore, we hypothesized that Exo-derived from chemo-resistant CC can contribute to the secretion of Nrf2 and thereby regulating the oxaliplatin sensitivity in Exo recipient cells. In the present study, we found that Nrf2 can be secreted via Exo, and exosomal Nrf2 can promote oxaliplatin resistance in CC cells via activation of the Nrf2/p-gp signaling pathways. Our results may provide new avenues for improving the effectiveness of oxaliplatin in treating CC.

2. Materials and Methods

2.1. Cell culture and expansion

Human colorectal cancer LS174T Cells were obtained from the Iranian Cell Bank (Pasteur Institute, Tehran, Iran). An oxaliplatin-resistant cell line (LS174T/R) was established from LS174T parental cell line (LS174T/S) as described previously [13, 14]. LS174T/S and LS174T/R cells were cultured in high-glucose content Dulbecco's modified Eagle's medium (DMEM/HG; Gibco, USA) culture medium at the standard condition in a humidified atmosphere with the temperature of 37°C and 5% CO_2. The medium was supplemented with 10% fetal bovine serum (FBS, Gibco) and 1% Penicillin/Streptomycin (Sigma-Aldrich, USA). Cells were subjected to different assays at passages between 3-6. For cell passage, cells were detached using 0.25% Trypsin-EDTA.

2.2. Exo isolation

In this study, Exo were extracted from the medium supernatant of LS174T/R and LS174T/S cells. To this end, cells were cultured in DMEM/HG with 10% Exo-depleted FBS for 48 hours. Upon 80-90% confluence, the supernatants were collected, and Exo were isolated by sequential centrifugations and ultracentrifugation steps as follows; In short, supernatants were centrifuged at 500 g for 30 minutes, 2000 g for 15 minutes, and at 10000 g for 30 minutes to exclude dead cells, apoptotic bodies, and non-Exo vesicles. Next, the supernatants were filtered using 0.22 μm microfilters (Millipore,

USA). In the next step, the samples were ultracentrifuged at 100,000 g for 1 hour at 4°C to precipitate exosomes (Optima ™ TLX, Beckman Coulter Inc., USA). Exosomal pellets were washed with cold phosphate-buffered saline (PBS) and ultracentrifuged under the same condition to reduce the possible protein contaminations. Finally, the exosomal pellets were resuspended in sterile PBS or distilled water and maintained at −80°C for the next steps. The protein content of Exo was quantified using the bicinchoninic acid (BCA; DNAbiotech, Iran) assay kit.

2.3. Dynamic light scattering

The Exo size distribution was analyzed by a laser-scattering technique. Briefly, the samples were diluted to 0.1 µg/µl using deionized water and sonicated for 10 minutes to achieve homogenous solutions [15]. Then, the size distribution of Exo was measured using a dynamic light scattering (DLS) device (Zetasizer Nano ZS90; Malvern Instruments, Malvern, UK).

2.4. Electron microscopy

Exo size and morphology were investigated by transmission electron microscopy (TEM). Briefly, isolated Exo were fixed in 2% glutaraldehyde overnight at 4°C. Then, a drop of Exo suspension was scattered on formvar/carbonated copper grids for 5 minutes, washed, counterstained with 2% uranyl acetate [16], and observed on a Zeiss LEO906 TEM (Jena, Germany).

2.5. Exo labeling and cellular uptake

Exo were extracted from the LS174T/R cell culture medium and labeled using fluorescent dye PKH26 (Sigma-Aldrich) according to the manufacturer's protocol. Thereafter, PKH26-labeled Exo and non-labeled Exo were co-incubated with LS174T cells in a complete culture medium for 24 hours. After completion of the incubation period, the plates were washed three times with PBS and fixed with 4% paraformaldehyde solution for 15 minutes. For nuclear staining, nuclei were stained with 4′,6-diamidino-2-phenylindole (DAPI; Sigma-Aldrich, USA), and the cells were visualized under Cytation™ 5 Cell Imaging Multi-Mode Reader (BioTek, USA).

2.6. Cell viability assay

Cell viability was evaluated via a colorimetric method using 3-(4,5-dimethylthiazol-2-yl)-2,5-diphenyltetrazolium Bromide (MTT; Sigma, USA). Briefly, pre-treated cells with different conditions were seeded in a 96-well plate (10,000/well) in triplicate for 24 hours. After incubation of the cells with a serial dilution of oxaliplatin, 20 µL of a 5 mg/ml MTT solution was added to each well and incubated for another 4 hours at 37°C. The medium was discarded and 200 µL of dimethyl sulfoxide (DMSO; Merck, Germany) was added. The plates were gently shacked for 15 minutes to dissolve the formazan crystals [13]. Finally, the optical density at 570 nm was measured by a microplate reader (Labsystems, Finland), and the IC50 was calculated on GraphPad Prism version 8.0.0 for Windows (GraphPad Software, USA).

2.7. Apoptosis assay

To this end, the LS174T/S and LS174T/R cells were seeded in six wells plate at a density of 100,000 cells/well. At an appropriate confluence, the cells were incubated with 10 µg/ml of Exo for 24 hours. Then, the media was removed and cells were exposed to IC_{50} of oxaliplatin for 48 hours. Finally, the cells were carefully harvested, washed with PBS, stained with Annexin V-FITC apoptosis detection kit (BD Biosciences, USA), and analyzed by using FACSCalibur flow cytometer (BD Biosciences, USA) and FlowJo (V10) software [13].

2.8. Western blot

Total cellular and exosomal proteins were extracted via a RIPA buffer (with a protease DNAbiotech, Iran) supplemented inhibitor cocktail (KALAZIST, Iran). Equal amounts of protein samples (determined by BCA assay) were separated on a 10% SDS-PAGE gel, transferred to PVDF membranes (Sigma, USA). Next, the membranes were blocked with 5% non-fat dry milk and incubated with primary antibodies against CD9 (sc-13118), CD63 (sc-5275), CD81 (sc-166029), Calnexin (sc-23954), Nrf2 (ab137550), P-gp (ab129450), MRP-1 (sc-18835), NQO1 (ab2346), HO1 (ab13248), and β-Actin (sc-47778; as a loading control) for 24 hours at 4°C. After that, the membranes were washed and incubated with appropriate HRP-conjugated secondary antibodies. The protein bands were detected by using an enhanced chemiluminescence

kit (ECL; Thermo Scientific, USA) on X-radiography films, and the density of bands were quantified by ImageJ software [17].

2.9. Real-time PCR (RT-qPCR) anaylsis

Total RNA from CC cell lines was extracted by using TRIzol reagent (Life Biolab, Germany) followed by reverse-transcription of RNA into cDNA using cDNA synthesis kit (Yekta Tajhiz, Iran) according to the manufacturer's protocols. RT-qPCR reaction was performed with SYBR green (Yekta Tajhiz, Iran) and LightCycler® 96 System (Roche Life Science, Italy). The following specific primer sequences were used for evaluation of each gene expression: Nrf2: F: 5′-TTC CCG GTC ACA TCG AGA G-3′ and GAPDH: F: 5′-GCA CCG TCA AGG CTG AGA AC-3′; R: 5′-TGG TGA AGA CGC CAG TGGA-3′. The $2^{-\Delta\Delta Ct}$ method was used to analysis of the gene expression. In the current study, GAPDH was used as the reference gene [13].

2.10. Colony formation assay

For this purpose, cells were seeded in 12-well plates at a density of 400 cells per well in 1 ml of completed media. After 24 hour-incubation of the cells with 400 nM of oxaliplatin, the medium was replaced with fresh media every 3 days. Twelve days later, the medium was discarded, cells were washed with PBS twice, fixed using 4% paraformaldehyde, stained with 0.1% crystal violet, washed with tap water, and counted visually [18].

2.11. Wound healing assay

Cells were seeded in six-well plates and allowed to create a single cell monolayer. Then, a scratch wound was made by using a sterile 100-µl pipette tip and wells were washed with sterile PBS to eliminate cells at the nude areas. Cells were treated with 10 µg/ml exosomal protein and incubated in a DMEM/HG medium containing 0.5% FBS for another 48 hours. Images were taken using an inverted microscope (Optika, Italy) at 0, 24, and 48 hours post-wounding and analyzed using ImageJ software [19].

2.12. Rhodamine 123 efflux assay

LS174T/S and Exo/R treated cells with a density of 3 × 10^5 cells/well were seeded in six-well plates and incubated in DMEM/HG culture medium with 10% FBS for 24 hours. Afterward, 1 mg/ml Rhodamine 123 (Rho-123; Sigma, USA) was added to each well and incubated at 37°C for 40 minutes, washed twice with PBS, resuspended in 500 µl ice-cold PBS, and analyzed with flow cytometer system (BD Biosciences, USA) and FlowJo software [17].

2.13. Statistical analysis

All data are expressed as mean ± SD analyzed by GraphPad Prism software version 8.0.0 for Windows (GraphPad Software, USA). Kolmogorov-Smirnov used to figure out the data distribution. Also, Student t-test and One-Way ANOVA tests were used to assess the difference between the two or more than two groups, respectively. $p < 0.05$ value was considered statistically significant.

3. Results

3.1. Nrf2 expression was increased in oxaliplatin-resistant cell line LS174T/R

To assess resistance in human colon cancer cells against oxaliplatin, we measured the IC_{50} values using the MTT assay in the two colon cell lines LS174T/S and LS174T/R. According to our data, the IC_{50} values in LS174T/S and of LS174T/R cells were 497.5 ± 13.61 nM and 8374 ± 285 nM, respectively, showing statistically significant difference between these cells ($p<0.001$, **Figure 1a-b**). Data exhibited that the resistance index (RI) of LS174T/R cells was 16.83. These data support the notion that oxaliplatin-resistant CC cells were successfully created by our protocol. RT-PCR and western blot assays showed the increased expression (5.4 fold) and protein levels (3.28 times) of Nrf2 in oxaliplatin-resistant cells compared to parental cells (**Figure 1c-e**). To evaluate the possible role of Nrf2 in the regulation of oxaliplatin resistance in CC, we inhibited the Nrf2 activity using a specific inhibitor namely brusatol (40 nM). MTT assay revealed that the oxaliplatin IC_{50} values reduced significantly in brusatol-treated cells (8.37 ± 0.19 µM) in comparison with non-treated LS174T/R cells (3.01 ± 0.07 µM**,** **Figure 1f-g**). In the next step, we found that treatment of LS174T/S cells with 20 µM tert-Butylhydroquinone (tBHQ), as an Nrf2 activator, increased the IC_{50} of oxaliplatin

(11.28 times, **Figure 1h-i**). These results showed that the Nrf2 inhibiting and activating can re-sensitize and desensitize LS174T CC cells to oxaliplatin, respectively.

3.2. Nrf2 is secreted via Exo into the culture medium

We isolated Exo from the culture medium of LS174T/R and LS174T/S cell lines as above-mentioned. TEM imaging showed that the isolated Exo possess a spherical to cup-shaped morphology with a bilayer membrane and a diameter reaching about 100 nm (**Figure 2a**). The purity of extracted Exo was examined by the DLS system (**Figure 2b**). DLS exhibited single populations in the Exo size range. Furthermore, exosomal surface markers such as CD9, CD63, and CD81 were characterized by western blot analysis (**Figure 2c**). Data showed that enriched Exo were positive for CD9, CD63, and CD81and negative for calnexin. As expected, western blot analysis revealed that Nrf2 was significantly increased in Exo fraction isolated LS174T/R cell culture supernatant compared control group ($p<0.001$, **Figure 2d-e**).

3.3. LS174T/R cell Exo promoted oxaliplatin resistance in parental cells

To illustrate the uptake of Exo by recipient cells, PKH26-labelled Exo isolated from LS174T/R (Exo/R) and LS174T/S (Exo/S) cells were incubated with LS174T/S cells. As shown in **Figure 3a**, Exo were successfully absorbed by the recipient cells and seen as red dots inside their cytoplasm. To select the optimal exosome concentration for subsequent experiments, LS174T cells were incubated with different concentrations of PKH26-labeled exosomes (0, 1, 2, 5, and 10 μg/ml) for 24 h, flow cytometry results showed that the highest fluorescent intensity was related to the concentration of 10 μg/ml. After 48-hour incubation of LS17T/S cells with Exo/R and Exo/S, we measured the IC_{50} values in the presence of oxaliplatin using MTT assay. Results showed that Exo/R significantly increased IC_{50} to oxaliplatin in LS174T/S cell compared to the group that received Exo/S (8.63 times, $p<0.001$, **Figure 3b-c**). However, the incubation of LS174T/S cells with Exo/S or Exo-depleted medium did not significantly alter the oxaliplatin sensitivity in these cells ($p>0.05$). Flow cytometry analysis revealed that apoptotic LS174T/S (29.32%) cells were significantly reduced after treatment with Exo/R (6.06%, $p<0.001$, **Figure 3d-e**). Taken together, these data suggest that Exo/R induced oxaliplatin resistance in human CC.

3.4. LS174T/R cell-derived Exo induced oxaliplatin resistance via regulation of Nrf2/p-glycoprotein axis

We hypothesized that exosomal Nrf2 is involved in oxaliplatin resistance. To validate this hypothesis, we examined the expression of Nrf2 was measured in recipient cells using western blotting. As shown in **Figure 4a-b**, Nrf2 levels were significantly increased in LS174T/S cells after incubation with Exo/R compared to the control group ($p<0.001$). based on our data, treatment with Brusatol re-sensitized Exo/R-treated LS174T/S cells to oxaliplatin (**Figure 4c-d**). In support of these findings, flow cytometry analysis confirmed that Nrf2 inhibition significantly enhanced the apoptotic LS174T/S cells (2.7 times, **Figure 4e-f**). Migration potential and colonization capacity are the two halmarks of chemoresistant cancer cells. As shown in **Figure 5a-d**, the treatment of LS174T/S cells with Exo/R significantly increased the clonogenic activity and promoted the wound closure compared matched-control group. Again, the suppression of Nrf2 with brusatol efficiently inhibited Exo/R‐induced clonogenic activity and migration potential. To further clarify the possible mechanism of exosome-mediated resistance to oxaliplatin in CC, we monitored the expressions of NAD(P)H quinone oxidoreductase 1 (NQO1) and heme oxygenase 1 (HO-1), and P-glycoprotein (P-gp) in Exo/R-treated LS174T/S cells as the main Nrf2 downstream target genes. We found that P-gp was significantly up-regulated in LS174T/S cells after in Exo/R-treated cells ($p<0.001$), but the expression of NQO1 and HO-1 did not show statistically significant changes ($p>0.05$; **Figure 6a-b**). To further evaluate the role of P-gp in Exo-mediated oxaliplatin resistance, we treated the Exo/R recipient cells with verapamil (10 μM) as a specific P-gp inhibitor. MTT and flow cytometry analyses revealed that P-gp inhibition re-sensitized Exo/R-treated cells to oxaliplatin (**Figure 6c-f**). Besides, a rhodamine 123 efflux assay revealed that Exo/R-treated cells exhibited higher P-gp activity indicated with lower intracellular Rho123 content. The exposure of Exo/R-treated cells led to the accumulation of Rho123 after the inhibition of P-gp function.

4. Discussion

CC is the third most common malignancy in both sexes worldwide. Oxaliplatin is one of the most effective anti-cancer agents used to treat CC. However, dose-dependent toxicity and the emergence of multidrug resistance limit its clinical application

in human medicine. Therefore, it is important to better understand the potential mechanisms involved in oxaliplatin resistance to identify promising targets for increasing the effectiveness of chemotherapy [1-3].

Here, we showed that oxaliplatin-resistant CC cells (LS174T/R) express higher levels of Nrf2 compared to sensitive counterparts (LS174T/S). Similarly, various studies have shown that Nrf2 is up-regulated in CC and many other cancers, and its increased expression is closely related to resistance against several chemotherapeutic agents [12, 13, 20-24]. We found that the inhibition and activation of Nrf2 by brusatol and tBHQ respectively decreased and increased resistance to oxaliplatin in LS174T/S cells, indicating the critical modulatory effect of Nrf2 in oxaliplatin resistance mechanisms. In line with our results, Payandeh et al. previously showed that the suppression of Nrf2 using siRNA can reduce the resistance of CC cells to oxaliplatin [25, 26]. So far, several mechanisms have been proposed for the promotion of resistance to anticancer agents. Recently, the critical role of Exo in chemoresistance has been introduced in the context of cancer [6]. Western blotting showed that LS174T/R cell-derived Exo can transfer higher levels of Nrf2 compared to their counterparts isolated from LS174T/R cell, indicating the fact that exosomal cargo is very similar to the cell of origin contents. Li et al. (2018) also showed that Exo isolated from adipose-derived stem cells overexpressing Nrf2 had higher levels of Nrf2 compared to parental cells [28]. These data show that any changes in the metabolic profile of source cells can be reflected in released Exo. In addition, our experiments showed that LS174T/R cell Exo can up-regulate Nrf2 expression, increased cell viability, colonization capacity, migration potential in LS174T/S cells. These features coincided with the reduction of apoptotic changes in these cells. Therefore, one can hypothesize that Exo are critical elements to induce resistance in acceptor cells. Interestingly, the inhibition of Nrf2 using brusatol in LS174T/R cell-derived Exo treated cells blunted these effects. These findings suggest that oxaliplatin-resistant cell-derived Exo containing Nrf2 can transmit the resistant phenotype to sensitive recipient cells. Similar to our results, Zhang et al. (2019) showed that exosomal transfer of p-STAT3 confers 5-FU resistance in colorectal cancer cells [29]. It has been shown that Exo-mediated transfer of chloride intracellular channel 1 (CLIC1) increases vincristine resistance in gastric cancers [30]. In another study, Exo

harboring ubiquitin carboxy-terminal hydrolase-L1 (UCH-L1) mediated Adriamycin resistance in breast cancer cells [31].

Concerning drug resistance in CC, several different proteins have been identified. For instance, P-gp is involved in drug resistance by pumping drugs out of the cell [32]. Some previous studies have shown P-gp expression is closely associated with the effectiveness of chemotherapy [10, 24, 33, 34] and that its expression is largely regulated by Nrf2 [35, 36]. To further elucidate the role of Nrf2 in the development of oxaliplatin resistance, we evaluated the expression of HO-1, NQO1, and P-gp in Exo/R treated sensitive cells. The western blot results showed that the expression of P-gp was closely associated with the level of Nrf2 in Exo recipient cells [37]. The inhibition of P-gp significantly reduced survival, increased apoptosis, and retention of rhodamine 123 in sensitive cells treated with Exo/R. These findings suggest that exosomal Nrf2 may enhance oxaliplatin resistance through modulating the expression of P-gp in recipient cells.

5. Conclusion

Commensurate with our data, Exo-mediated transfer of Nrf2 may be involved in the development of oxaliplatin resistance by increasing P-gp expression in recipient cells. However, further *in vitro* and *in vivo* studies are needed to confirm these results.

Abbreviations

ARE; antioxidant response elements, BCA; bicinchoninic acid, CC; colon cancer, CLIC1; Chloride intracellular channel 1, DMEM; Dulbecco's modified Eagle's medium, DMSO; dimethyl sulfoxide, DLS; dynamic light scattering, FBS; fetal bovine serum, FOLFOX; l-leucovorin and 5-fluorouracil, HO-1; heme oxygenase 1, IC50; half maximal inhibitory concentration, Keap1; Kelch-like ECH-associated protein 1, MTT; 3-(4,5-dimethylthiazol-2-yl)-2,5-diphenyltetrazolium Bromide, Nrf2; Nuclear factor erythroid 2-related factor 2, NQO1; NAD(P)H quinone oxidoreductase 1, 1-OHP; Oxaliplatin, PBS; phosphate-buffered saline, RTPCR; Reverse transcriptase-polymerase chain reaction,

tBHQ; tert-Butylhydroquinone, TME; tumor microenvironment, TEM; transmission electron microscopy, UCH-L1; ubiquitin carboxy-terminal hydrolase-L1.

Acknowledgments We special thanks to the Drug Applied Research Center for their assistance in the progression of my thesis.

Authors' contributions NS and MN supervised and managed the research. HK, and SH analyzed and interpreted the results of the experiments. MM conceived, designed, and performed the experiments, analyzed data, and drafted the manuscript. All authors read and approved the final manuscript.

Funding This work was financially supported by the Drug Applied Research Center and Research Vice-Chancellor of Tabriz University of Medical Sciences, Tabriz, Iran. (Ph.D. Thesis No. 59755) and Iran National Science Foundation (INSF) (Grant No. 97014455).

Availability of data and materials All data generated or analyzed during this study are included in this published article.

Ethics approval and consent to participate This study protocol was approved by the Ethics Committee of the Tabriz University of medical sciences, Tabriz, Iran (IR.TBZMED.VCR.REC.1397.117).

Consent for publication Not applicable.

Competing interests The authors declare that they have no conflict of interest.

References:

1. Sung, H., et al., *Global cancer statistics 2020: GLOBOCAN estimates of incidence and mortality worldwide for 36 cancers in 185 countries.* CA: a cancer journal for clinicians, 2021. **71**(3): p. 209-249.
2. Deng, X., et al., *A KLF4/PiHL/EZH2/HMGA2 regulatory axis and its function in promoting oxaliplatin-resistance of colorectal cancer.* Cell death & disease, 2021. **12**(5): p. 1-13.
3. Ning, T., et al., *Exosomal miR-208b related with oxaliplatin resistance promotes Treg expansion in colorectal cancer.* Molecular Therapy, 2021.

4. Jena, B.C. and M. Mandal, *The emerging roles of exosomes in anti-cancer drug resistance and tumor progression: An insight towards tumor-microenvironment interaction.* Biochimica et Biophysica Acta (BBA)-Reviews on Cancer, 2020: p. 188488.
5. Kahroba, H., M.S. Hejazi, and N. Samadi, *Exosomes: from carcinogenesis and metastasis to diagnosis and treatment of gastric cancer.* Cellular and Molecular Life Sciences, 2019. **76**(9): p. 1747-1758.
6. Mostafazadeh, M., et al., *Potential roles and prognostic significance of exosomes in cancer drug resistance.* Cell & Bioscience, 2021. **11**(1): p. 1-15.
7. Zhou, J., et al., *Tumor-derived exosomes in colorectal cancer progression and their clinical applications.* Oncotarget, 2017. **8**(59): p. 100781.
8. Hu, Y.-B., et al., *Exosomal Wnt-induced dedifferentiation of colorectal cancer cells contributes to chemotherapy resistance.* Oncogene, 2019. **38**(11): p. 1951-1965.
9. Kahroba, H. and Y. Davatgaran-Taghipour, *Exosomal Nrf2: From anti-oxidant and anti-inflammation response to wound healing and tissue regeneration in aged-related diseases.* Biochimie, 2020. **171**: p. 103-109.
10. Jeddi, F., et al., *Contradictory roles of Nrf2/Keap1 signaling pathway in cancer prevention/promotion and chemoresistance.* DNA repair, 2017. **54**: p. 13-21.
11. Gong, J. and H. Xu, *Current Perspectives on the Role of Nrf2 in 5-Fluorouracil Resistance in Colorectal Cancer.* Anti-cancer Agents in Medicinal Chemistry, 2021.
12. Sadeghi, M.R., et al., *The role of Nrf2-Keap1 axis in colorectal cancer, progression, and chemoresistance.* Tumor Biology, 2017. **39**(6): p. 1010428317705510.
13. Tazehkand, A.P., et al., *The role of Her2-Nrf2 axis in induction of oxaliplatin resistance in colon cancer cells.* Biomedicine & Pharmacotherapy, 2018. **103**: p. 755-766.
14. McDermott, M., et al., *In vitro development of chemotherapy and targeted therapy drug-resistant cancer cell lines: a practical guide with case studies.* Frontiers in oncology, 2014. **4**: p. 40.
15. Lyu, T.S., et al., *The characterization of exosomes from fibrosarcoma cell and the useful usage of Dynamic Light Scattering (DLS) for their evaluation.* Plos one, 2021. **16**(1): p. e0231994.
16. Ren, R., et al., *Colon cancer cells secrete exosomes to promote self-proliferation by shortening mitosis duration and activation of STAT3 in a hypoxic environment.* Cell & bioscience, 2019. **9**(1): p. 1-9.

17. Haiaty, S., et al., *Thymoquinone inhibited vasculogenic capacity and promoted mesenchymal-epithelial transition of human breast cancer stem cells.* BMC Complementary Medicine and Therapies, 2021. **21**(1): p. 1-12.
18. Zhang, H.W., et al., *Cancer-associated fibroblast-derived exosomal microRNA-24-3p enhances colon cancer cell resistance to MTX by down-regulating CDX2/HEPH axis.* Journal of Cellular and Molecular Medicine, 2021. **25**(8): p. 3699-3713.
19. Shirafkan, N., et al., *microRNA-193a-5p inhibits migration of human HT-29 colon cancer cells via suppression of metastasis pathway.* Journal of cellular biochemistry, 2019. **120**(5): p. 8775-8783.
20. Akhdar, H., et al., *Involvement of Nrf2 activation in resistance to 5-fluorouracil in human colon cancer HT-29 cells.* European journal of cancer, 2009. **45**(12): p. 2219-2227.
21. Homma, S., et al., *Nrf2 enhances cell proliferation and resistance to anticancer drugs in human lung cancer.* Clinical Cancer Research, 2009. **15**(10): p. 3423-3432.
22. Jiang, T., et al., *High levels of Nrf2 determine chemoresistance in type II endometrial cancer.* Cancer research, 2010. **70**(13): p. 5486-5496.
23. Lee, Y.J., et al., *Overexpression of Nrf2 promotes colon cancer progression via ERK and AKT signaling pathways.* Annals of surgical treatment and research, 2020. **98**(4): p. 159.
24. Sadeghi, M.R., et al., *Nrf2/P–glycoprotein axis is associated with clinicopathological characteristics in colorectal cancer.* Biomedicine & Pharmacotherapy, 2018. **104**: p. 458-464.
25. Payandeh, Z., et al., *The Potential Role of Nrf2-PD-L1 Axis in Promoting of Oxaliplatin Resistance in Colon Cancer Cells.* 2020.
26. Payandeh, Z., et al., *The Impact of Nrf2 Silencing on Nrf2-PD-L1 Axis to Overcome Oxaliplatin Resistance and Migration in Colon Cancer Cells.* Avicenna Journal of Medical Biotechnology, 2021. **13**(3): p. 117.
27. Wan, Z., et al., *Exosome-mediated cell-cell communication in tumor progression.* American journal of cancer research, 2018. **8**(9): p. 1661.
28. Li, X., et al., *Exosomes from adipose-derived stem cells overexpressing Nrf2 accelerate cutaneous wound healing by promoting vascularization in a diabetic foot ulcer rat model.* Experimental & molecular medicine, 2018. **50**(4): p. 1-14.
29. Zhang, Q., et al., *Exosomal transfer of p-STAT3 promotes acquired 5-FU resistance in colorectal cancer cells.* Journal of Experimental & Clinical Cancer Research, 2019. **38**(1): p. 1-14.

30. Zhao, K., et al., *Exosome-mediated transfer of CLIC1 contributes to the vincristine-resistance in gastric cancer.* Molecular and cellular biochemistry, 2019. **462**(1): p. 97-105.
31. Ning, K., et al., *UCH-L1-containing exosomes mediate chemotherapeutic resistance transfer in breast cancer.* Journal of surgical oncology, 2017. **115**(8): p. 932-940.
32. Hu, T., et al., *Mechanisms of drug resistance in colon cancer and its therapeutic strategies.* World journal of gastroenterology, 2016. **22**(30): p. 6876.
33. Baekelandt, M.M., et al., *P-glycoprotein expression is a marker for chemotherapy resistance and prognosis in advanced ovarian cancer.* Anticancer research, 2000. **20**(2B): p. 1061-1067.
34. Kato, T., et al. *Serum exosomal P-glycoprotein is a potential marker to diagnose docetaxel resistance and select a taxoid for patients with prostate cancer*. in *Urologic Oncology: Seminars and Original Investigations*. 2015. Elsevier.
35. Jeddi, F., et al., *Nrf2 overexpression is associated with P-glycoprotein upregulation in gastric cancer.* Biomedicine & Pharmacotherapy, 2018. **97**: p. 286-292.
36. Wu, B., et al., *Nrf2 overexpression protects against paraquat-induced A549 cell injury primarily by upregulating P-glycoprotein and reducing intracellular paraquat accumulation.* Experimental and therapeutic medicine, 2019. **17**(2): p. 1240-1247.
37. Summers, M.A., J.L. Moore, and J.W. McAuley, *Use of verapamil as a potential P-glycoprotein inhibitor in a patient with refractory epilepsy.* Annals of Pharmacotherapy, 2004. **38**(10): p. 1631-1634.

Figure legends

Fig. 1. The role of Nrf2 in CC oxaliplatin resistance. (a and b) The viability of LS174T/S and LS174T/R cells was measured by MTT assay after treatment with different concentrations of oxaliplatin for 72 h. (c, d, and e) The mRNA and protein level of Nrf2 was determined using RT-PCR and western blot methods in both LS174T/S and LS174T/R cells. The LS174T/R cells express higher levels of Nrf2 (mRNA and Protein) in comparison to LS174T/S cells. (f-i) The cells were treated with either brusatol (40 nM) or tBHQ (20 μM) for 2 h followed by treatment with different concentrations of oxaliplatin for 72 h. Data are expressed in Mean ± SD and representative of three independent experiments. ***$p < 0.001$ vs. LS174T/R cells.

Fig. 2. Increased expression of Nrf2 in exosomes isolated from oxaliplatin resistant CC cells. (a) TEM micrographs of exosomes isolated from LS174T/S or LS174T/R cells. Scale bar, 100 nm. (b) The exosomes size distribution was analyzed by the DLS technique. The size distribution of isolated exosomes was in the range of 50-50 nm. (c) Exosomal markers CD9, CD63, and CD81 were characterized by western blot analysis. These exosomal protein markers were expressed in the exosomes but not in the conditioned medium. In contrast, calnexin (non-exosomal marker) was only observed in the conditioned medium and not in the exosome fraction. (d and e) Quantitative analysis of Nrf2 protein expression in Exo/S and Exo/R. Beta-actin was used as an endogenous loading control. The Exo/R had higher levels of Nrf2 (Protein) in comparison to Exo/S. ***P <0.001.

Fig. 3. LS174T/R derived exosomes transfer oxaliplatin resistance in CC. (a) Isolated exosomes labeled with PKH26 (red dye) were added to LS174T cells. Scale bar represents 100 μm. (b and c) Cell viability assays were performed in LS174T/S cells treated with exosome depleted conditioned medium (C.M), Exo/R, or Exo/S and a range of oxaliplatin concentrations for 72 h. (d and e) Annexin V/PI apoptosis assays were performed in LS174T/S and Exo/R-treated LS174T/S cells for 48 h. Data are expressed in Mean ± SD and representative of three independent experiments.

Fig. 4. Exosomal transfer of Nrf2 enhances oxaliplatin resistance. (a and b) Western blot analysis of Nrf2 in LS174T/S and Exo/R-treated LS174T/S cells. Beta-actin was used as an endogenous reference. (c and d) MTT assay and IC_{50} values (72 h) of LS174T cells to oxaliplatin in the Exo/R and Exo/R + brusatol (Bru, 40 nM) groups. (e and f) Flow cytometry analysis of apoptosis in LS174T cells pre-incubated with Exo/R or Exo/R + Bru (40 nM) followed by oxaliplatin treatment for 48 hr. All data are expressed in Mean ± SD and representative of three independent experiments. **P <0.01 and ***P <0.001.

Fig. 5. Exosome-mediated delivery of Nrf2 increases the colony formation ability and wound healing potential in recipient cells. (a and b) Colony formation assay in LS174T/S

cells treated with PBS, Exo/R, or Exo/R + Bru (40 nM). (c and d) Wound healing assay in LS174T/S cells treated with PBS, Exo/R, or Exo/R + Bru (40 nM) at 0, 24, and 48 hr. All values are expressed in Mean ± SD and representative of three independent experiments. Differences between the three groups were analyzed using the ANOVA test. ***P < 0.001

Fig. 6. Exosomal Nrf2 enhances P-gp expression in recipient cells. (a and b) Western blot analysis of HO-1, NQO1, and P-gp as the main Nrf2 downstream target genes in LS174T/S and Exo/R-treated LS174T/S cells. In contrast to NQO1 and HO-1, P-gp expression significantly increased in LS174T/S cells after co-culturing with Exo/R. (c and d) MTT assay and IC_{50} values (72 h) of LS174T cells to oxaliplatin in the Exo/R and Exo/R + Verapamil (Ver, 10 μM) groups. (e and f) Flow cytometry analysis of apoptosis in LS174T cells pre-incubated with Exo/R or Exo/R + Ver (10 μM) followed by oxaliplatin treatment for 48 hr. (g and h) Rho 123 efflux assay was carried out to determine the P-gp activity in the exosome-treated cells. Exo/R-treated cells showed lower fluorescence intensity (FI) in comparison to LS174T/S cells. Data represent Mean ± SD. of three independent experiments; ***P < 0.001 vs. LS174T/S and $^{###}p < 0.001$ vs. LS174T/S + Exo/R groups.

Fig. 7. Schematic representation of exosomal Nrf2 in regulating oxaliplatin resistance. The schematic illustration showed how exosomes from oxaliplatin-resistant CC cells mediated resistance in the sensitive ones.

Figure legends

Fig. 1. The role of Nrf2 in CC oxaliplatin resistance. (a and b) The viability of LS174T/S and LS174T/R cells was measured by MTT assay after treatment with different concentrations of oxaliplatin for 72 h. (c, d, and e) The mRNA and protein level of Nrf2 was determined using RT-PCR and western blot methods in both LS174T/S and LS174T/R cells. The LS174T/R cells express higher levels of Nrf2 (mRNA and Protein) in comparison to LS174T/S cells. (f-i) The cells were treated with either brusatol (40 nM) or tBHQ (20 μM) for 2 h followed by treatment with different concentrations of oxaliplatin for 72 h. Data are expressed in Mean ± SD and representative of three independent experiments. ***$p < 0.001$ vs. LS174T/R cells.

Fig. 2. Increased expression of Nrf2 in exosomes isolated from oxaliplatin resistant CC cells. (a) TEM micrographs of exosomes isolated from LS174T/S or LS174T/R cells. Scale bar, 100 nm. (b) The exosomes size distribution was analyzed by the DLS technique. The size distribution of isolated exosomes was in the range of 50 50 nm. (c) Exosomal markers CD9, CD63, and CD81 were characterized by western blot analysis. These exosomal protein markers were expressed in the exosomes but not in the conditioned medium. In contrast, calnexin (non-exosomal marker) was only observed in the conditioned medium and not in the exosome fraction. (d and e) Quantitative analysis of Nrf2 protein expression in Exo/S and Exo/R. GAPDH was used as an endogenous loading control. The Exo/R had higher levels of Nrf2 (Protein) in comparison to Exo/S. ***$P < 0.001$.

Fig. 3. LS174T/R derived exosomes transfer oxaliplatin resistance in CC. (a) Isolated exosomes labeled with PKH26 (red dye) were added to LS174T cells. Scale bar represents 100 μm. (b and c) Cell viability assays were performed in LS174T/S cells treated with exosome depleted conditioned medium (C.M), Exo/R, or Exo/S and a range of oxaliplatin concentrations for 72 h. (d and e) Annexin V/PI apoptosis assays were performed in LS174T/S and Exo/R-treated LS174T/S cells for 48 h. Data are expressed in Mean ± SD and representative of three independent experiments.

Fig. 4. Exosomal transfer of Nrf2 enhances oxaliplatin resistance. (a and b) Western blot analysis of Nrf2 in LS174T/S and Exo/R-treated LS174T/S cells. Beta-actin was used as an endogenous reference. (c and d) MTT assay and IC_{50} values (72 h) of LS174T cells to oxaliplatin in the Exo/R and Exo/R + brusatol (Bru, 40 nM) groups. (e and f) Flow cytometry analysis of apoptosis in LS174T cells pre incubated with Exo/R or Exo/R + Bru (40 nM) followed by oxaliplatin treatment for 48 hr. All data are expressed in Mean ± SD and representative of three independent experiments. **P <0.01 and ***P <0.001.

Fig. 5. Exosome-mediated delivery of Nrf2 increases the colony formation ability and wound healing potential in recipient cells. (a and b) Colony formation assay in LS174T/S cells treated with PBS, Exo/R, or Exo/R + Bru (40 nM). (c and d) Wound healing assay in LS174T/S cells treated with PBS, Exo/R, or Exo/R + Bru (40 nM) at 0, 24, and 48 hr. All values are expressed in Mean ± SD and representative of three independent experiments. Differences between the three groups were analyzed using the ANOVA test. ***P < 0.001

Fig. 6. Exosomal Nrf2 enhances P-gp expression in recipient cells. (a and b) Western blot analysis of HO-1, NQO1, and P-gp as the main Nrf2 downstream target genes in LS174T/S and Exo/R-treated LS174T/S cells. In contrast to NQO1 and HO-1, P-gp expression significantly increased in LS174T/S cells after co-culturing with Exo/R. (c and d) MTT assay and IC_{50} values (72 h) of LS174T cells to oxaliplatin in the Exo/R and Exo/R + Verapamil (Ver, 10 μM) groups. (e and f) Flow cytometry analysis of apoptosis in LS174T cells pre incubated with Exo/R or Exo/R + Ver (10 μM) followed by oxaliplatin treatment for 48 hr. (g and h) Rho 123 efflux assay was carried out to determine the P-gp activity in the exosome-treated cells. Exo/R-treated cells showed lower fluorescence intensity (FI) in comparison to LS174T/S cells. Data represent Mean ± SD. of three independent experiments; ***P < 0.001 vs. LS174T/S and $^{###}p < 0.001$ vs. LS174T/S + Exo/R groups.

Fig. 7. Schematic representation of exosomal Nrf2 in regulating oxaliplatin resistance. The schematic illustration showed how exosomes from oxaliplatin-resistant CC cells mediated resistance in the sensitive ones.

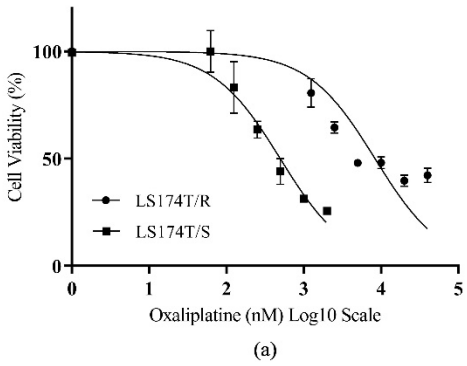
Cell Viability (%)
100
50
0
LS174T/R
LS174T/S
0 1 2 3 4 5
Oxaliplatine (nM) Log10 Scale

(a)

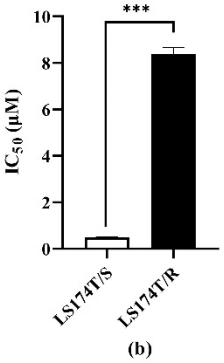
***
IC50 (µM)
10
8
6
4
2
0
LS174T/S
LS174T/R

(b)

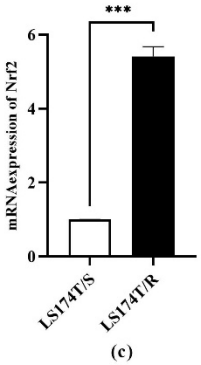
***
mRNAexpression of Nrf2
6
4
2
0
LS174T/S
LS174T/R

(c)

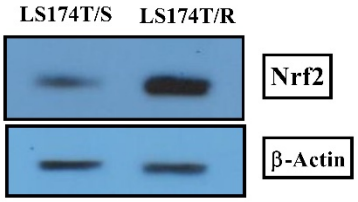
LS174T/S
LS174T/R
Nrf2
β-Actin

(d)

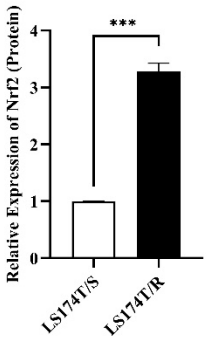
***
Relative Expression of Nrf2 (Protein)
4
3
2
1
0
LS174T/S
LS174T/R

(e)

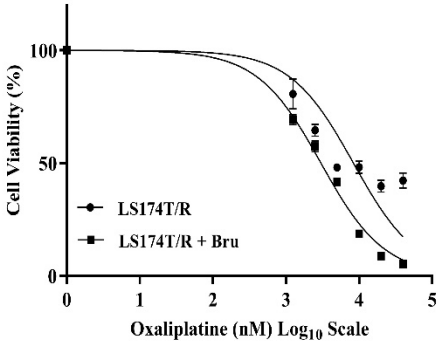
Cell Viability (%)
100
50
0
LS174T/R
LS174T/R + Bru
0 1 2 3 4 5
Oxaliplatine (nM) Log10 Scale

(f)

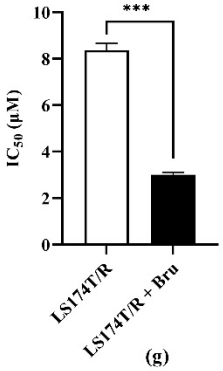
***
IC50 (µM)
10
8
6
4
2
0
LS174T/R
LS174T/R + Bru

(g)

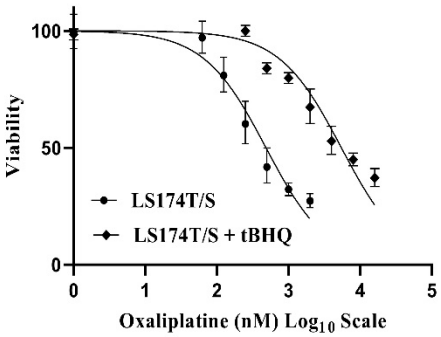
Viability
100
50
0
LS174T/S
LS174T/S + tBHQ
0 1 2 3 4 5
Oxaliplatine (nM) Log10 Scale

(h)

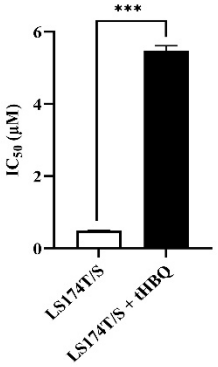
***
IC50 (µM)
6
4
2
0
LS174T/S
LS174T/S + tHBQ

(i)

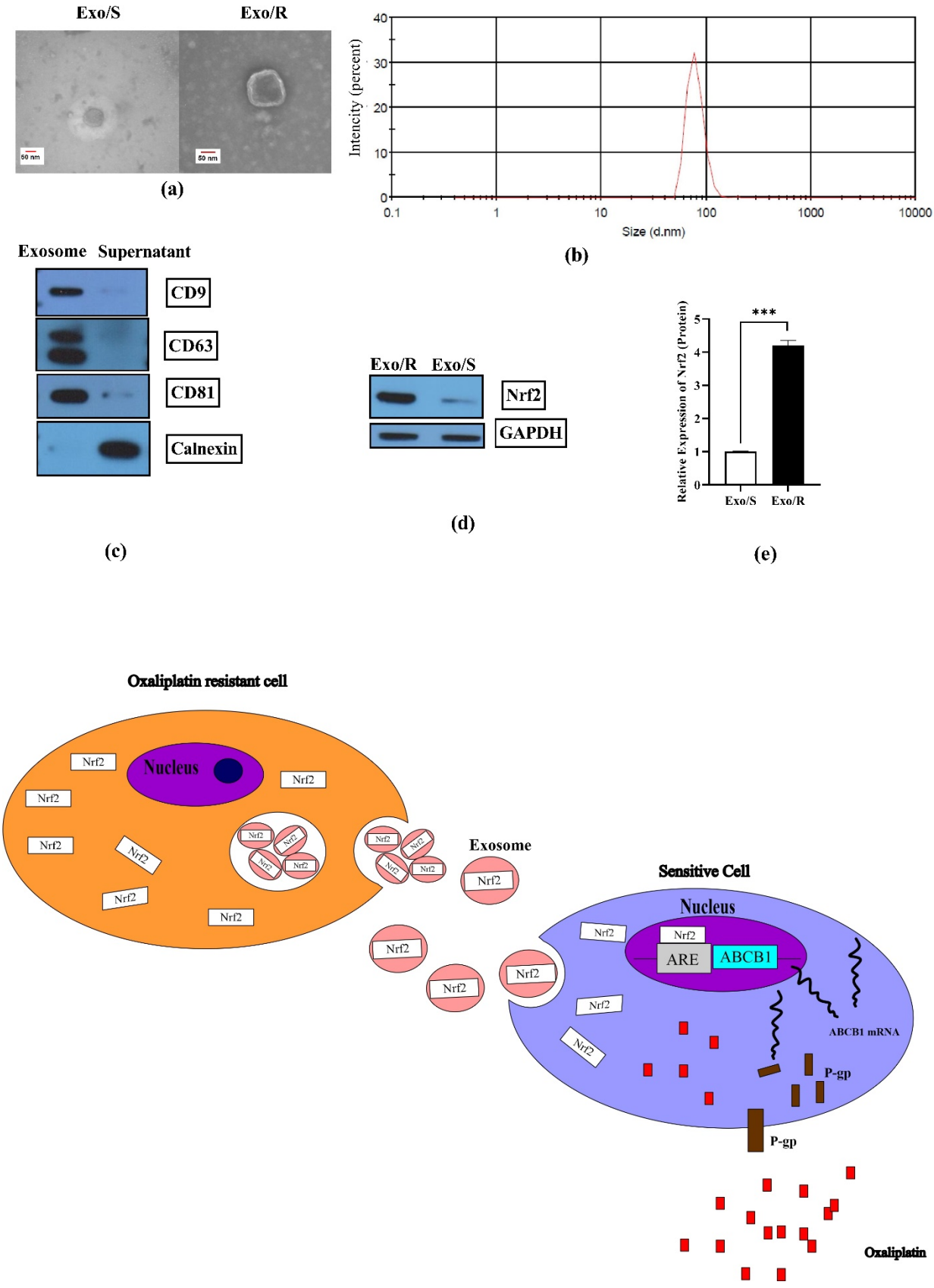
Exo/S
Exo/R
50 nm
50 nm
(a)
Intencity (percent)
40
30
20
10
0
0.1
1
10
100
1000
10000
Size (d.nm)
(b)
Exosome
Supernatant
CD9
CD63
CD81
Calnexin
(c)
Exo/R
Exo/S
Nrf2
GAPDH
(d)
***
Relative Expression of Nrf2 (Protein)
5
4
3
2
1
0
Exo/S
Exo/R
(e)
Oxaliplatin resistant cell
Nucleus
Nrf2
Exosome
Sensitive Cell
Nucleus
ARE
ABCB1
ABCB1 mRNA
P-gp
P-gp
Oxaliplatin

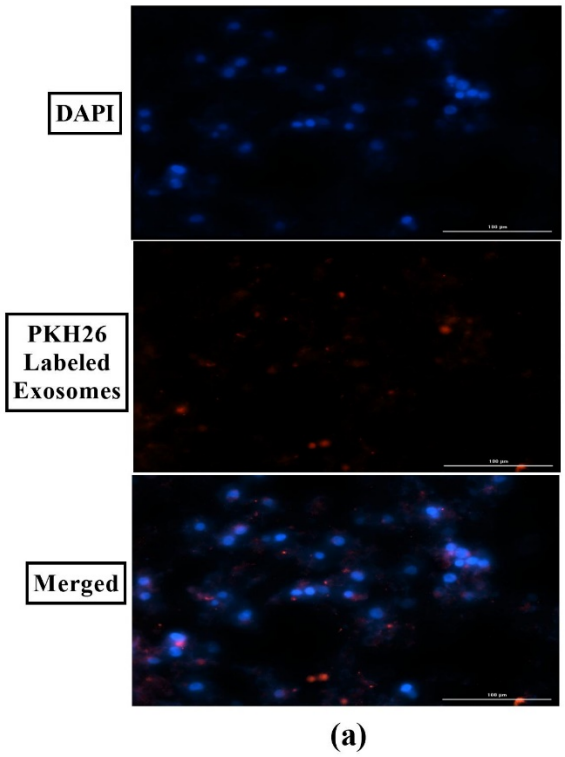
DAPI
PKH26 Labeled Exosomes
Merged

(a)

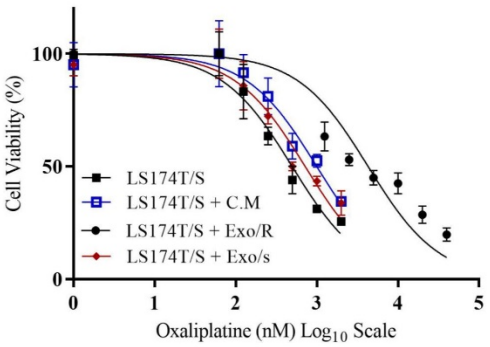
Cell Viability (%)
100
50
0
0
1
2
3
4
5
LS174T/S
LS174T/S + C.M
LS174T/S + Exo/R
LS174T/S + Exo/s
Oxaliplatine (nM) Log10 Scale

(b)

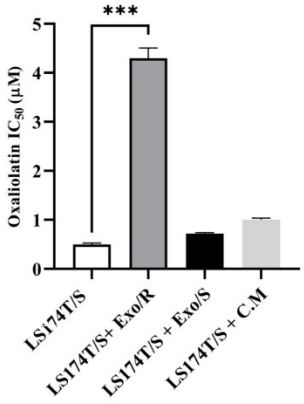
***
Oxaliolatin IC50 (μM)
5
4
3
2
1
0
LS174T/S
LS174T/S+ Exo/R
LS174T/S + Exo/S
LS174T/S + C.M

(c)

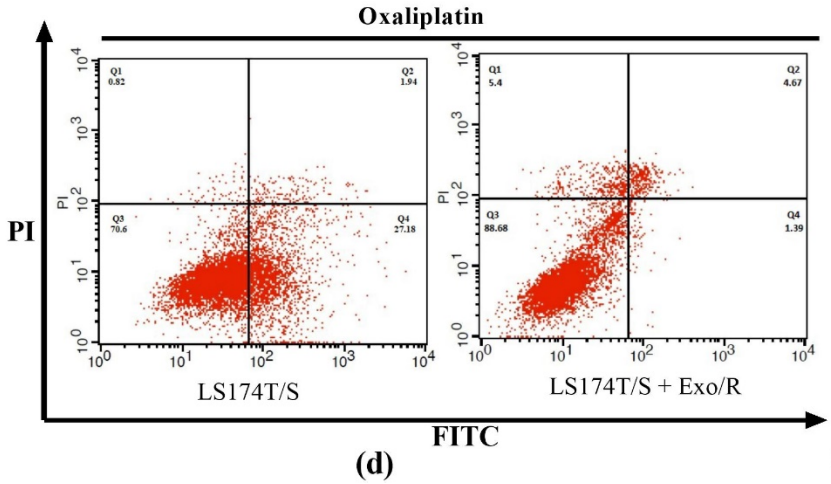
Oxaliplatin
PI
Q1
0.82
Q2
1.94
Q3
70.6
Q4
27.18
Q1
5.4
Q2
4.67
Q3
88.68
Q4
1.39
LS174T/S
LS174T/S + Exo/R
FITC

(d)

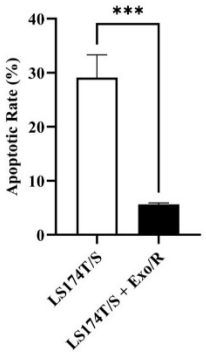
***
Apoptotic Rate (%)
40
30
20
10
0
LS174T/S
LS174T/S + Exo/R

(e)

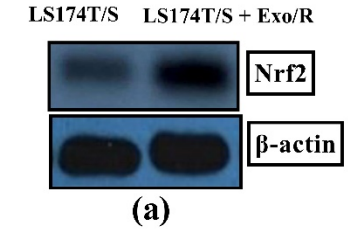
LS174T/S
LS174T/S + Exo/R
Nrf2
β-actin

(a)

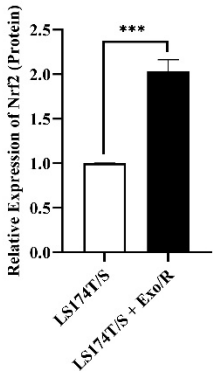
Relative Expression of Nrf2 (Protein)
***
LS174T/S
LS174T/S + Exo/R

(b)

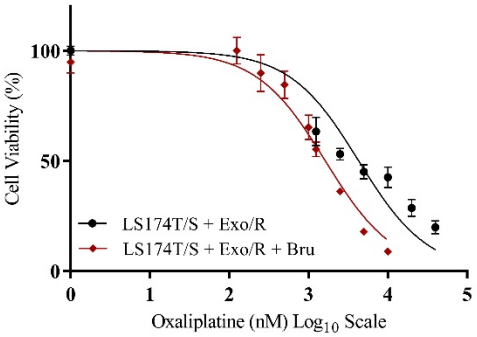
Cell Viability (%)
LS174T/S + Exo/R
LS174T/S + Exo/R + Bru
Oxaliplatine (nM) Log10 Scale

(c)

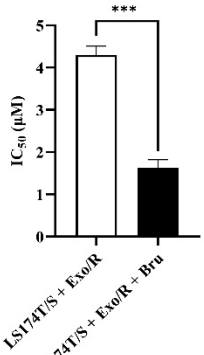
IC50 (μM)
***
LS174T/S + Exo/R
LS174T/S + Exo/R + Bru

(d)

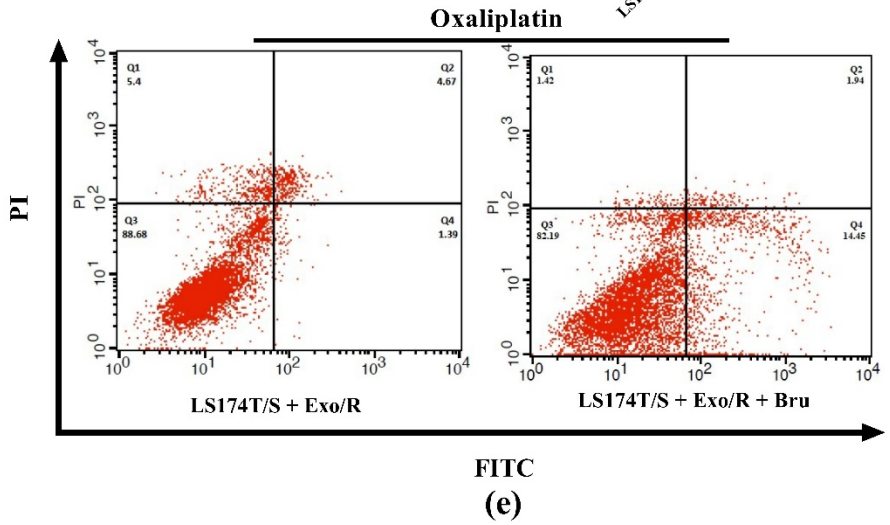
Oxaliplatin
PI
Q1
5.4
Q2
4.67
Q3
88.68
Q4
1.39
Q1
1.42
Q2
1.94
Q3
82.19
Q4
14.45
LS174T/S + Exo/R
LS174T/S + Exo/R + Bru
FITC

(e)

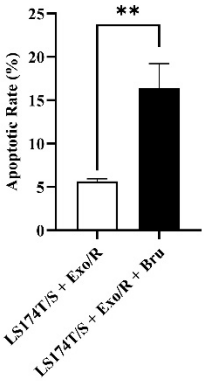
Apoptotic Rate (%)
**
LS174T/S + Exo/R
LS174T/S + Exo/R + Bru

(f)

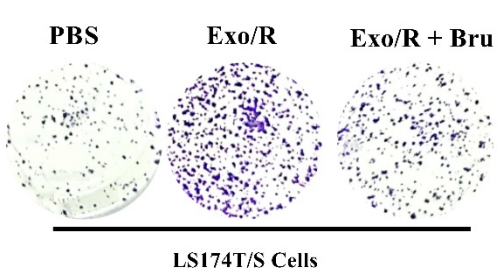
PBS
Exo/R
Exo/R + Bru
LS174T/S Cells

(a)

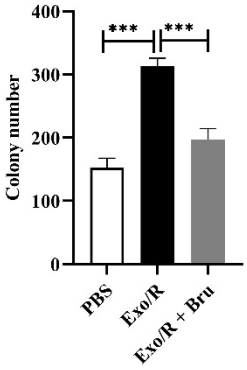
Colony number
400
300
200
100
0
***
***
PBS
Exo/R
Exo/R + Bru

(b)

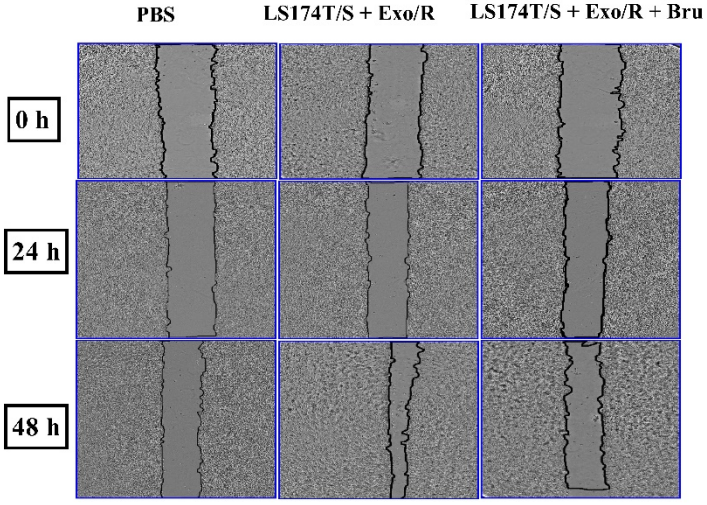
PBS
LS174T/S + Exo/R
LS174T/S + Exo/R + Bru
0 h
24 h
48 h

(e)

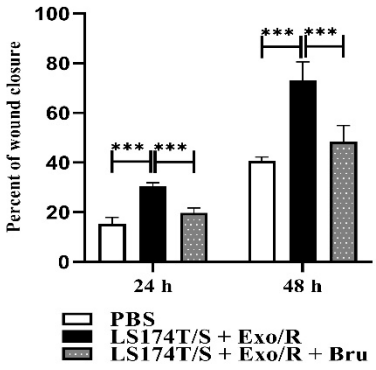
Percent of wound closure
100
80
60
40
20
0
***
***
***
***
24 h
48 h
PBS
LS174T/S + Exo/R
LS174T/S + Exo/R + Bru

(d)

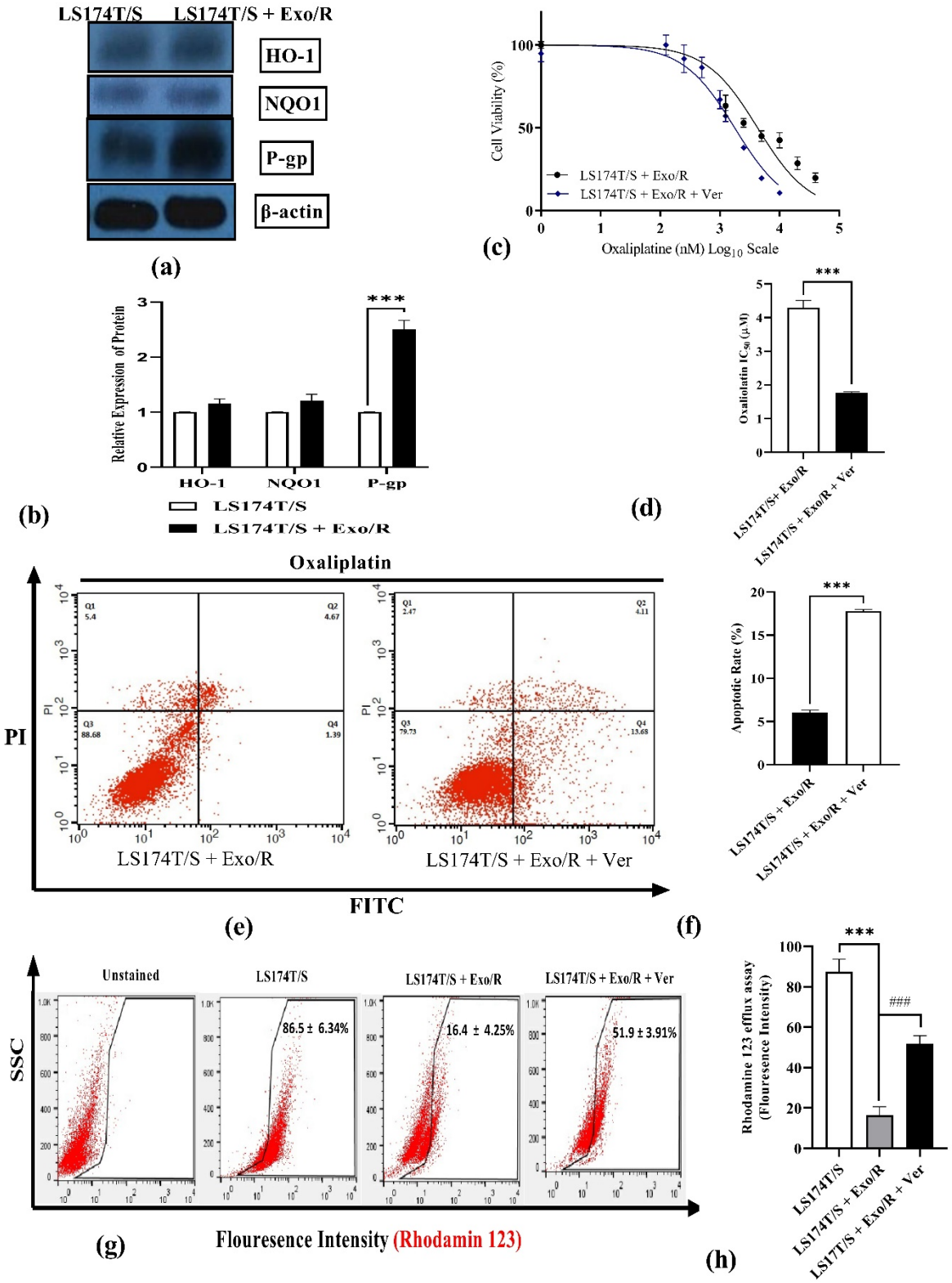
LS174T/S
LS174T/S + Exo/R
HO-1
NQO1
P-gp
β-actin
(a)
Cell Viability (%)
LS174T/S + Exo/R
LS174T/S + Exo/R + Ver
Oxaliplatine (nM) Log10 Scale
(c)
Relative Expression of Protein
***
HO-1
NQO1
P-gp
LS174T/S
LS174T/S + Exo/R
(b)
Oxaliolatin IC50 (μM)
***
LS174T/S+ Exo/R
LS174T/S + Exo/R + Ver
(d)
Oxaliplatin
PI
FITC
Q1 5.4
Q2 4.67
Q3 88.68
Q4 1.39
Q1 2.47
Q2 4.11
Q3 79.73
Q4 13.68
LS174T/S + Exo/R
LS174T/S + Exo/R + Ver
(e)
Apoptotic Rate (%)
***
LS174T/S + Exo/R
LS174T/S + Exo/R + Ver
(f)
Unstained
LS174T/S
LS174T/S + Exo/R
LS174T/S + Exo/R + Ver
SSC
86.5 ± 6.34%
16.4 ± 4.25%
51.9 ± 3.91%
Flouresence Intensity (Rhodamin 123)
(g)
Rhodamine 123 efflux assay (Flouresence Intensity)
***
###
LS174T/S
LS174T/S + Exo/R
LS17T/S + Exo/R + Ver
(h)